

SURFACE SPIN WAVES IN ANTIFERROMAGNETIC NiO

R. E. De Wames and T. Wolfram

Science Center, North American Rockwell Corporation, Thousand Oaks, California 91360

(Received 2 December 1968)

Interpretation of the temperature dependence of exchange-scattered low-energy electrons leads to the prediction of a low-lying surface-spin-wave band in antiferromagnetic NiO.

Exchange scattering of low-energy electrons from antiferromagnetic NiO has been reported recently by Palmberg, De Wames, and Vredetoe.¹ Theoretically the cross section for this scattering is proportional to the square of the thermal average of the z component of the spin of the scattering atom, $\langle S_z \rangle^2$.² Because low-energy electrons penetrate only a few atomic layers,³ the intensity of the exchange-scattered electrons is expected to depend strongly on the sublattice magnetization of only the surface spins. Experimental measurement² of the temperature dependence of the intensity of exchange-scattered electrons from NiO indicates that the temperature dependence of the surface sublattice magnetization departs considerably from the bulk behavior as deduced from neutron-scattering experiments.⁴ A simple molecular-field calculation, reported elsewhere,² which takes into account surface corrections yields a temperature dependence for the surface sublattice magnetization which is in good qualitative agreement with that observed experimentally, provided the exchange interaction between spins on the surface is smaller than the bulk exchange. The purpose of this note is (1) to point out that the above-mentioned results strongly imply the existence of low-lying surface-spin-wave states in NiO, (2) to show that a simple Heisenberg model for an antiferromagnet predicts the existence of such surface states for reasonable values of the surface exchange parameters, and (3) to show that these low-lying surface states are characterized by very flat dispersion curves, a feature necessary for the validity of the molecular-field model.

In contrast to electrons, neutrons penetrate deeply into a crystal and consequently the cross section for neutrons scattered by the atomic dipole moment is proportional to the square of the thermal average of the bulk magnetization. The temperature dependence of the cross sections for neutron dipole scattering⁴ and electron exchange scattering from NiO are shown in Fig. 1. The upper curve, for neutrons, follows the temperature dependence of the bulk magnetization

while the lower curve, for electrons, displays a different behavior. Lack of low-temperature data prohibits a quantitative comparison of these two experimental curves. Nevertheless, the qualitative features of these two curves are quite different. The neutron curve shows a convex curvature, as expected from the thermal behavior of the bulk magnetization, while the curve for the electrons clearly displays a concave curvature. As mentioned earlier, this concave nature can be explained by a molecular-field model provided that the surface exchange is assumed to be smaller than that of the bulk. The results of the molecular-field calculation are illustrated in Fig. 2.

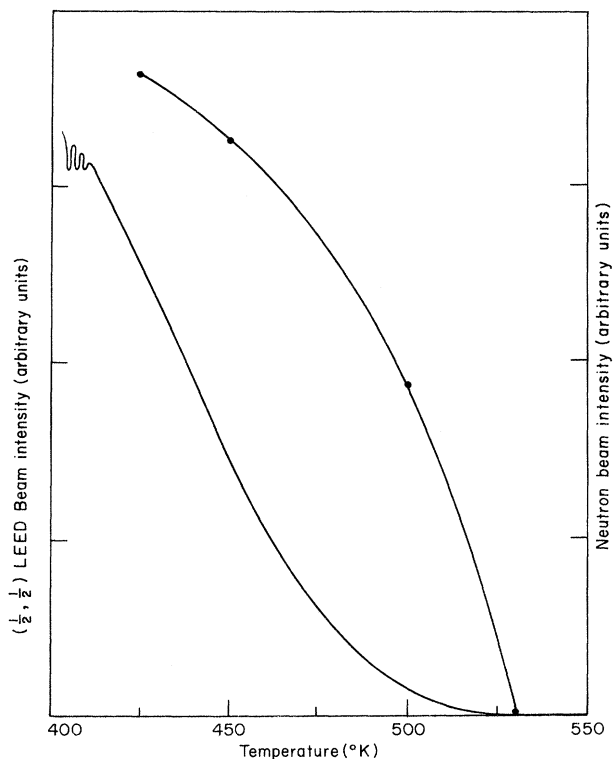


FIG. 1. Temperature dependence of neutron and electron scattering intensities. The upper curve is the (111) neutron beam intensity observed by Roth, Ref. 4. The lower curve is the $(\frac{1}{2}, \frac{1}{2})$ electron beam intensity, Ref. 2.

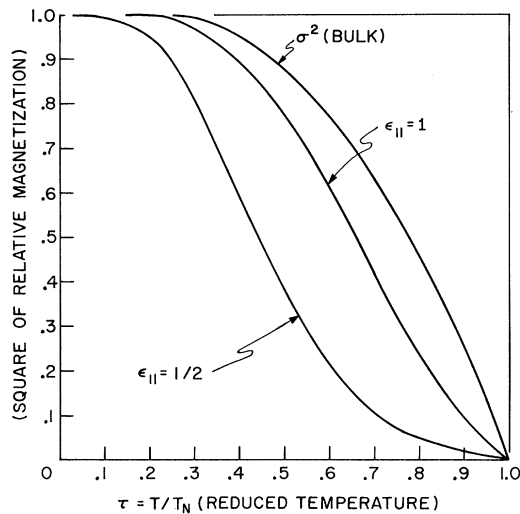


FIG. 2. The square of the sublattice magnetization according to the molecular-field model. The upper curve is the bulk result and the two lower curves are for the surface layer with different values for the exchange parameters.

The upper curve is the square of the sublattice magnetization for an infinite antiferromagnet which according to the molecular-field model is

given by the Brillouin function for $S = 1$. This curve is similar to the neutron data of Fig. 1. The lower two curves of Fig. 2 are the molecular-field results for the surface spins of a semi-infinite sample for different values of the surface exchange parameter J_{\parallel} . The curve for $\epsilon_{\parallel} = J_{\parallel}/J = \frac{1}{2}$, where J is the bulk exchange parameter, possesses a concave curvature similar to that exhibited by the electron cross-section curve of Fig. 1. We find that a reasonable reduction of the surface exchange leads, according to the Heisenberg model, to the existence of low-energy antiferromagnetic surface-spin-wave states.⁵ These states are eigenstates of the perturbed antiferromagnet and may be characterized as plane waves propagating parallel to the surface and attenuated with increasing depth into the crystal.⁶

In order to illustrate the features of the antiferromagnetic surface-spin-wave states we consider the [100] surface of a two-sublattice antiferromagnet with simple cubic structure and restrict the calculation to zero temperature, $T = 0$. For spin S , anisotropy energy h , and $C = JS$, the surface spin-wave energy E is given by

$$(E/C)^2 = (6 + h/C)^2 - [4/(1 - y^2)] - (\gamma_k^2/y^2), \quad (1)$$

where y is a root of the cubic equation

$$(6C + h)\Delta\omega_0 y^3 - (C^2 + \Delta\omega_1^2 - \Delta\omega_0^2 - \omega_1\Delta\omega_1)y^2 - [\Delta\omega_1^2 - \Delta\omega_0^2 - C^2 + (6C + h)\Delta\omega_0]y - \omega_1\Delta\omega_1 = 0, \quad (2)$$

with the parameters defined as

$$\begin{aligned} \gamma_k &= \sum_{\vec{\Delta}_{\parallel}} \exp(i\vec{k} \cdot \vec{\Delta}_{\parallel}), \\ \omega_1 &= C\gamma_k, \\ \Delta\omega_0 &= C[1 + Z_{\parallel}(1 - \epsilon_{\parallel})] + \Delta h, \\ \Delta\omega_1 &= (1 - \epsilon_{\parallel})\omega_1, \end{aligned} \quad (3)$$

where Z_{\parallel} is the number of nearest "in-plane" neighbors, Δh is the change in the anisotropy energy, and the sum over $\vec{\Delta}_{\parallel}$ is over nearest neighbors in a plane parallel to the surface. One of the roots of the cubic equation corresponds to a surface spin wave but the other two roots do not give physical solutions. In Fig. 3 we show the square of the surface-state energy as a function of the parameter $4 - \gamma_k$ for a simple cubic structure for several values of surface exchange ratio ϵ_{\parallel} . For simplicity the curves are presented for

structure for several values of surface exchange ratio ϵ_{\parallel} . For simplicity the curves are presented for

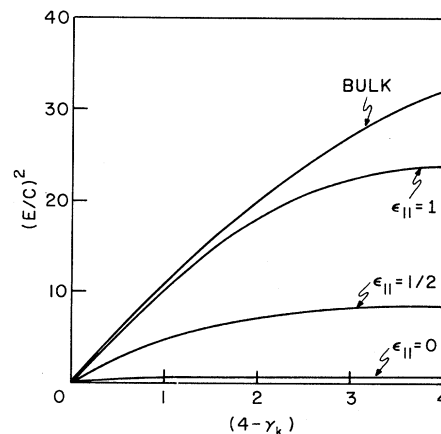


FIG. 3. Dependence of the square of the surface spin-wave energy on the parameter γ_k for different values of ϵ_{\parallel} .

$\hbar = 0$. The upper curve is for a bulk spin wave in an infinite antiferromagnet with a propagation vector having a vanishing component normal to the surface. Examination of the eigenvectors of these states shows that the amplitude of the spin excitation decreases in a complicated exponential manner with increasing depth into the crystal.⁶ In general, the rate of decrease of excitation amplitude increases with increasing E for fixed ϵ_{\parallel} and also increases for decreasing ϵ_{\parallel} at fixed E . The surface modes have excitation energies lower than that of the corresponding bulk states and consequently lead to a more rapid decrease in the surface magnetization. The surface modes are also characterized by very flat dispersion curves. This feature suggests that over much of k space the surface-spin-wave band could be approximated by a single excitation level and it is just this circumstance that is required for the validity of a molecular-field model.

It is interesting to note that surface waves exist for the antiferromagnet with nearest-neighbor coupling even for the case in which there is no perturbation in the surface exchange or surface anisotropy field, while in the case of the ferromagnet such perturbations are necessary in order to produce surface states.⁷

At finite temperatures additional terms enter

the equations for the surface states so that the surface-spin-wave dispersion curves depend upon temperature in manner more complicated than the usual thermal energy renormalization.

¹P. W. Palmberg, R. E. De Wames, and L. A. Vredevoe, *Phys. Rev. Letters* **21**, 682 (1968).

²P. W. Palmberg, R. E. De Wames, L. A. Vredevoe, and T. Wolfram, to be published.

³E. G. MacRae, *J. Chem. Phys.* **45**, 3258 (1966).

⁴W. L. Roth, *Phys. Rev.* **111**, 772 (1958).

⁵The spectrum for antiferromagnetic surface spin waves on the [100] surface of a bcc crystal (which has spins of only one sublattice on the surface) has been derived by Mills and Saslow for the case in which the surface exchange is unperturbed; see D. L. Mills and W. M. Saslow, *Phys. Rev.* **171**, 448 (1968). Since exchange scattering from antiferromagnetics can be observed only from surfaces containing spins of both sublattices and since the effect of the reduced surface exchange is of central importance here, it is necessary to develop more general expressions.

⁶In the case of a surface containing spins of both sublattices the surface-state eigenvectors are quite complex. The amplitude of excitation depends upon two functions which decrease exponentially with distance from the surface as well as a sublattice structure factor.

⁷B. N. Filippov, *Fiz. Tverd. Tela* **9**, 1339 (1967) [translation: *Soviet Phys.-Solid State* **9**, 1048 (1967)].

EFFECT OF NUCLEAR DEFORMATION ON FAST-NEUTRON TOTAL CROSS SECTIONS*

Dale W. Glasgow and D. Graham Foster, Jr.

Battelle Memorial Institute, Pacific Northwest Laboratory, Richland, Washington

(Received 25 November 1968)

We have observed the effect of nuclear deformation on the fast-neutron total cross sections of 15 deformed nuclei within the region $152 \leq A \leq 189$, and five deformed nuclei within the region $228 \leq A \leq 240$. The phenomenological nonlocal optical model of Perey and Buck disagrees in these regions with our experimental data.

We have finished a large-scale program¹ of measurements of fast-neutron total cross sections for 78 naturally occurring elements and 14 separated isotopes. The measurements included all of the elements from H to Pu with the exception of the six inert gases and the highly radioactive elements near radium. The cross sections were measured with a pulsed-beam time-of-flight system at about 240 different energies per element to a statistical precision varying from

2.0 to 0.6% for $3.0 \leq E_n \leq 15.0$ MeV and an energy resolution of 2.5 to 4.5% over the same limits. Previous measurements were essentially nonexistent over this energy range for the heavier alkali metals and alkaline earths, rare and expensive metals, the rare earths, various actinides, and most of the 14 separated isotopes. A detailed analysis of the data will be published shortly.

We emphasize the point that the large range in